JOURNAL OF THERMOPHYSICS AND HEAT TRANSFER
Vol. 25, No. 3, July–September 2011

Technical Notes

Shape Optimization of Inclined Elliptic Dimples in a Cooling Channel

Hyun-Min Kim,* Mi-Ae Moon,* and Kwang-Yong Kim†
Inha University, Incheon 402-751, Republic of Korea

DOI: 10.2514/1.T3674

Nomenclature

A	=	area of heat transfer, mm^2
D_h	=	hydraulic diameter of the channel, mm
d_a	=	average diameter of the ellipse, $(d_1 + d_2)/2$, mm
d_1	=	major diameter of the ellipse, mm
d_2	=	minor diameter of the ellipse, mm
F	=	objective function
F_f	=	objective function related to the pressure drop
F_{Nu}	=	objective function related to the heat transfer
f	=	friction factor of the channel
H	=	height of the channel, mm
H_d	=	dimple depth, mm
k	=	fluid thermal conductivity, W/m · K
Nu	=	Nusselt number
Nu_a	=	area-averaged Nusselt number
P	=	streamwise distance between the dimples, mm
Pr	=	Prandtl number
q	=	wall heat flux, 600 W/m^2
Re	=	Reynolds number, $U_b D_h/v$
S	=	spanwise distance between the dimples, mm
T_b	=	bulk temperature, K
T_w	=	wall temperature, K
U_b	=	average velocity at the inlet, m/s
x, y, z	=	orthogonal coordinate system
α	=	angle of major diameter to the streamwise directions, θ
Δp	=	pressure drop, Pa
v	=	kinematic viscosity, m^2/s
ρ	=	fluid density, kg/m^3

I. Introduction

DIMPLES have been widely applied in many heat-exchanging devices, such as heat exchangers, cooling devices for electronic components, and internal cooling channels of turbine blades. Dimples are usually attached periodically on the heat transfer surface, and cause the development of vortices and turbulence to enhance convective heat transfer. As a heat transfer augmentation device, dimples have an advantage of a small pressure drop compared with the other devices such as ribs, pin-fins, and protrusions, because they do not directly block the main flow.

Many researches have been conducted both numerically and experimentally to reveal the characteristics of the flowfield and heat transfer in cooling channels with circular dimples. Hwang et al. [1] experimentally investigated dimples and protrusions. They showed that dimples induce lower pressure drop but higher heat transfer than protrusions. Ligrani et al. [2] investigated the effect of dimple depth. They observed that the length scale of a vortex downstream of a dimple increases with the dimple depth. Isaev and Leont'ev [3] performed a numerical study in a dimpled channel. They suggested that the heat transfer enhances as the dimple depth increases, and the flowfield and heat transfer patterns in a dimple are changed at a specific depth of the dimple.

Various noncircular shapes of dimples have been also studied by many researchers. Moon and Lau [4] experimentally investigated characteristics of a cylindrical dimpled channel. Their results showed that cylindrical dimples have higher heat transfer performance than circular dimples. Park and Ligrani [5] numerically analyzed the heat transfer performances of seven dimple shapes. They suggested that the highest heat transfer is induced by circular and inclined cylindrical dimples. Silva et al. [6] studied characteristics of elliptic dimples in laminar flow ($Re = 500$–1000). The heat transfer performance is highest when the major axis of the ellipse is normal to the flow direction. Vicente et al. [7] performed an experimental study on a cooling channel with elliptic dimples placed helically. Through a parametric study, they showed that the heat transfer and pressure loss increase with the dimple depth. But the pitch does not have remarkable affect on the cooling performance. Isaev et al. [8] have studied circular and inclined oval dimples to find the effects of dimple depth, dimple diameter, and Reynolds number.

Shape optimization of a circular dimpled channel has been already conducted by Kim et al. [9] and Samad et al. [10] using Reynolds-averaged Navier–Stokes (RANS) analysis and surrogate models. As the design variables, they selected the ratio of the channel height to the dimple diameter, ratio of the dimple depth to the diameter, and ratio of the dimple diameter to the pitch between the dimples. However, optimization of noncircular dimples has not been conducted, yet.

In this study, optimization of a cooling channel with inclined elliptic dimples based on three-dimensional RANS analysis has been performed to enhance the heat transfer and reduce the pressure loss in the channel. A radial basis neural network (RBNN) model [11] has been used to construct the surrogate for the optimization. Three design variables are related to the elliptic dimple shape, viz., the ratio of the channel height to the dimple diameter, ratio of the dimple depth to the diameter, and angle of ellipse major axis to flow direction.

II. Numerical Analysis

Figure 1 shows the geometry of the cooling channel to be analyzed in this study. The channel aspect ratio is 3.0 and the hydraulic diameter is 22.5 mm. A total of 14 dimples (seven rows) are placed parallel in the computational domain. The inlet of the computational domain is located 73 mm away from the leading edge of the first row of the dimples and the outlet at 88 mm from the trailing edge of the last row of the dimples.

For the flowfield and heat transfer analyses, three-dimensional continuity, RANS, and energy equations are solved using the commercial code ANSYS CFX 11.0 [12], which employs an unstructured grid system. As boundary conditions, uniform velocity profile is applied at the inlet with Reynolds number 10,000 based on the channel hydraulic diameter. A constant-pressure condition is set as the outlet condition. On the walls, a constant heat flux (600 W/m^2) is applied with a no-slip condition. The working fluid is air at 25°C.

The low-Reynolds-number shear stress transport (SST) model [13] is employed as the turbulence closure. The SST turbulent model is a combination of the k-ε and k-ω models; the k-ω model is adopted

Received 5 January 2011; revision received 4 April 2011; accepted for publication 6 April 2011.

*Graduate Student, Department of Mechanical Engineering, 253 Yonghyun-Dong, Nam-Gu.

†Professor, Department of Mechanical Engineering, 253 Yonghyun-Dong, Nam-Gu; kykim@inha.ac.kr. Associate Fellow AIAA.

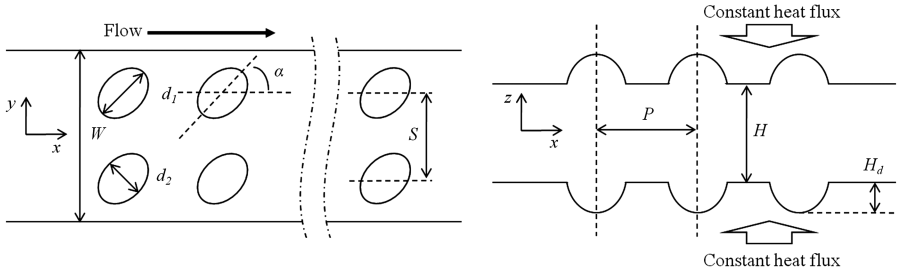

a) Top view **b) Side view**

Fig. 1 Geometric parameters and computational domain.

in the near-wall region, and the k-ε model is adopted n the other region. Furthermore, the SST model calculates transport of turbulent shear stress between the k-ε and k-ω models. Samad et al. [10] showed that the SST model well predicts the flow and heat transfer in a dimpled cooling channel, in comparison with the experimental results.

Unconstructed tetrahedral grids are used with prism layers near the wall. To adopt the low-Reynolds-number version of the SST model (k-ω model) in the near-wall region, first grid points from the wall are placed at $0.0003H$ to satisfy $y+$ less than 1.0. A grid-dependency test has been conducted to find optimum number of the grids in the range of from 700,000 to 2,700,000. Through the grid-dependency test, 1,600,000 has been selected as the optimal number of grids in this study. Samad et al. [14,15] performed shaped optimization of a cooling channel with various dimples to enhance heat transfer, and the results of RANS analysis with the same numerical methods as in this work showed good agreements with the experimental data for Nusselt number distribution on the heat transfer surface.

The root-mean-squared relative residual values of all variables were maintained at less than $1.0e-6$ as the criterion of convergence of the solutions. The solutions converged after approximately 600 iterations. The average computational time was about 4 h using an eight-part local parallel mode with an Intel i7 2.67 GHz CPU.

III. Optimization Procedure

The channel height (H), channel width (W), dimple average diameter ($d_a = (d_1 + d_2)/2$), ratio of ellipse diameters (d_2/d_1), angle of major diameter of the dimple to the flow direction (α), dimple depth (H_d), streamwise distance of dimples (S), and spanwise distance of dimples (P) are the geometric parameters of the channel considered. From these parameters, three nondimensional design variables, viz., the ratio of ellipse diameters (d_2/d_1), ratio of dimple depth to average diameter (H_d/d_a), and angle of major diameter of the dimple to the flow direction (α), were selected for the optimization. Table 1 shows the range of each design variable for the present optimization. The design ranges were decided from a preliminary parametric study. Twenty-one design points (experimental points) for the surrogate model were selected by Latin hypercube sampling [16] in this study. The objective-function value at each design point was obtained by RANS analysis.

The objective function is defined as a linear combination of a heat-transfer-related and friction-loss-related terms with a weighting factor β as follows:

$$F = F_{Nu} + \beta F_f \tag{1}$$

Table 1 Design variables and design space

	Design variables		
	d_2/d_1	H_d/d_a	α
Lower bound	0.5	0.1	60°
Upper bound	1.0	0.3	90°

where the weighting factor β is a parameter that is determined by the designer.

The heat-transfer-related term F_{Nu} is the inverse of the area-averaged Nusselt number:

$$F_{Nu} = 1/Nu_a \tag{2}$$

where

$$Nu_a = \frac{\int_A Nu/Nu_0 \, \mathrm{d}A}{A} \qquad Nu = \frac{\dot{q}D_h}{k(T_w - T_b)}$$

$$Nu_0 = 0.023Re^{0.8}Pr^{0.4}$$

where Nu_a is the area-averaged Nusselt number. A is the heat transfer area in the dimpled channel. Nu_0 is the Dittus–Boelter correlation, which indicates the Nusselt number in a smooth pipe.

The friction-loss-related term F_f is defined as follows:

$$F_f = (f/f_0)^{1/3} \tag{3}$$

$$f = \frac{\Delta p D_h}{2\rho U_b^2 P} \qquad f_0 = 2(2.236 \ln Re - 4.639)^{-2}$$

where f indicates the friction factor in the channel, and f_0 is the friction factor in a smooth pipe.

The RBNN [11] is a two-layered network with a hidden layer of radial basis transfer function with linear output. The hidden layer consists of a set of radial basis functions that act as activation function, the response of which varies with the distance between the input and the center. The distance between two points is determined by the difference of their coordinates and by a set of parameters. The main advantage of using the radial basis approach is the ability to reduce the computational cost, due to the linear nature of the radial basis functions. The linear model F can be expressed as a linear combination of a set of N basis functions:

$$F(x) = \sum_{j=1}^{N} w_j y_j \tag{4}$$

where w_j is the weight and y_j is a basis function. The weight w_j indicates the contribution of the basis function y_j to the respective output unit. The ability of the network for prediction is stored in the weight that can be obtained from a set of training patterns. In the present study, a customized RBNN function, i.e., `newrb`, available in MATLAB was used. Once the RBNN model is constructed by using the objective-function values at the design points, the optimum point is searched by sequential quadratic programming.

IV. Results and Discussion

As an example of the optimization, the optimization for $\beta = 0.09$ has been performed and the results are represented in Table 2. The RBNN model predicts that the objective-function value of the

Table 2 Results of optimization for $\beta = 0.09$

	Design variables					F	
	d_2/d_1	H_d/d_a	α	F_{Nu}	F_f	RBNN	RANS
Reference	1.000	0.300	90.00	0.598	1.412	——	0.725
Optimum	0.575	0.280	62.33	0.330	1.859	0.504	0.497

optimum design is 0.504. This value has only 1.3% relative error compared with the objective-function value obtained by RANS analysis. The optimum design of the inclined elliptic dimples in the channel produces 31.4% reduction in the objective-function value compared with the reference design. The value of area-averaged Nusselt number for the optimum design is 3.03, which is the value increased by 81.2% compared with the reference design. The friction factor of the optimum design is also increased by 31.7% compared with the reference design. Two design variables of the optimum design, d_2/d_1 and α, are located near the lower boundaries of the corresponding design ranges, but H_d/d_a is located near the upper boundary.

Figure 2 shows the local Nusselt number distributions on the dimpled surfaces. Low heat transfer regions are found in the front parts of the dimple, and the heat transfer rate increases to approach the peak values near the rear rims in both of the dimple shapes. The low heat transfer regions are occurred by the flow separation at the front rims of the dimples and the heat transfer increases by flow reattachment in the rear part of the dimples as depicted in the previous work [9]. The heat transfer rate increases as the flow proceeds downstream through the dimple rows in both cases. The optimum inclined elliptic dimples show obviously higher level of the overall Nusselt number than the reference circular shape. The maximum heat transfer regions are found near the rear rim on the right of the flow direction. The distribution of Nusselt number for the reference shape (Fig. 2a) shows the asymmetric pattern, even though the geometry is symmetric. This asymmetry is induced by the asymmetric flow structure, as Isaev and Leonnt'ev [17] suggested that turbulent flow passing a deep circular dimple causes asymmetric vortex structure. The local Nusselt number distributions along a streamwise line (centerline of the dimple in the case of the circular shape) through the

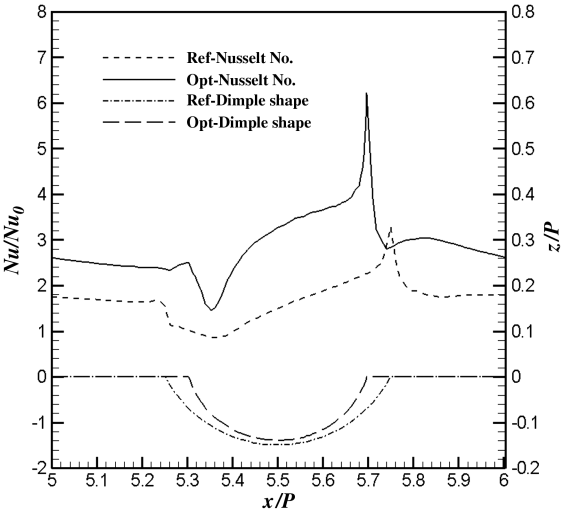

Fig. 3 Local Nusselt number distributions along a streamwise line ($y/W = 0.25$) through the sixth dimple row.

sixth dimple row are represented in Fig. 3. The local Nusselt number of the optimum shape is much higher than that of the reference shape on most of the dimpled surface. And the peak Nusselt number of the optimum shape is nearly two times larger than that of the reference shape. The difference in Nusselt number between the two cases is pronounced on the dimple surface, rather than on the surface between dimples. The increase in the Nusselt number of the optimum shape takes place more rapidly than that of the reference shape in the front part of the dimple.

Figure 4 shows the velocity vectors on the planes normal to the flow direction, A–A' and B–B'. On the plane A–A', a big cross-stream vortex is generated near the center of the dimple in both cases. However, the vortex is much stronger in the case of the optimum shape than with the reference shape. Unlike the case of the reference shape, the strong vortex in the optimum dimple persists along the side wall downstream of the dimple (plane B–B'). This strong three-dimensional flow structure enhances the heat transfer, as shown in Fig. 3

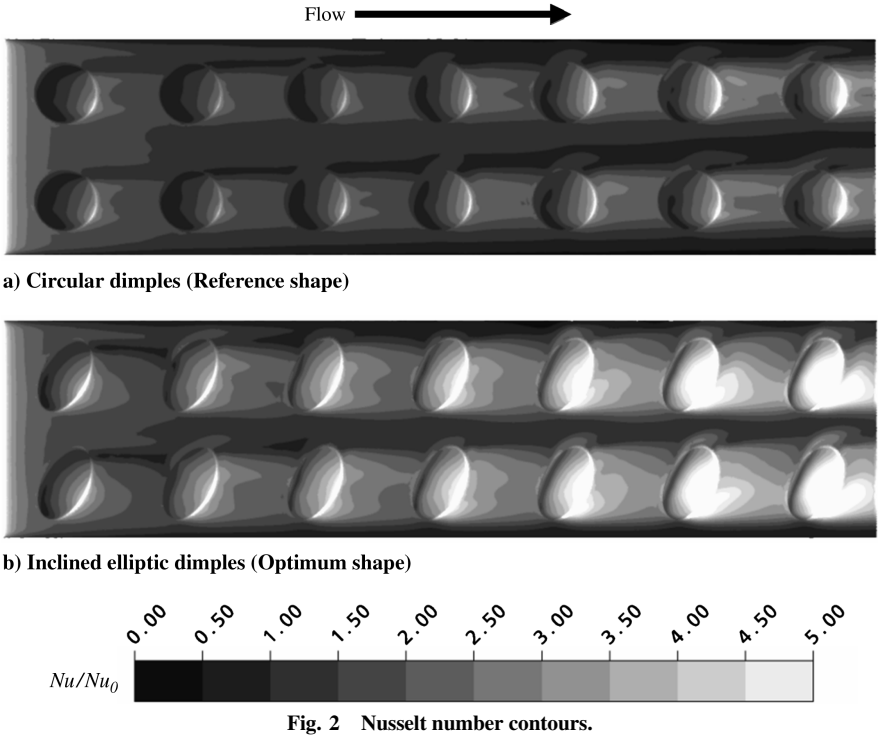

Fig. 2 Nusselt number contours.

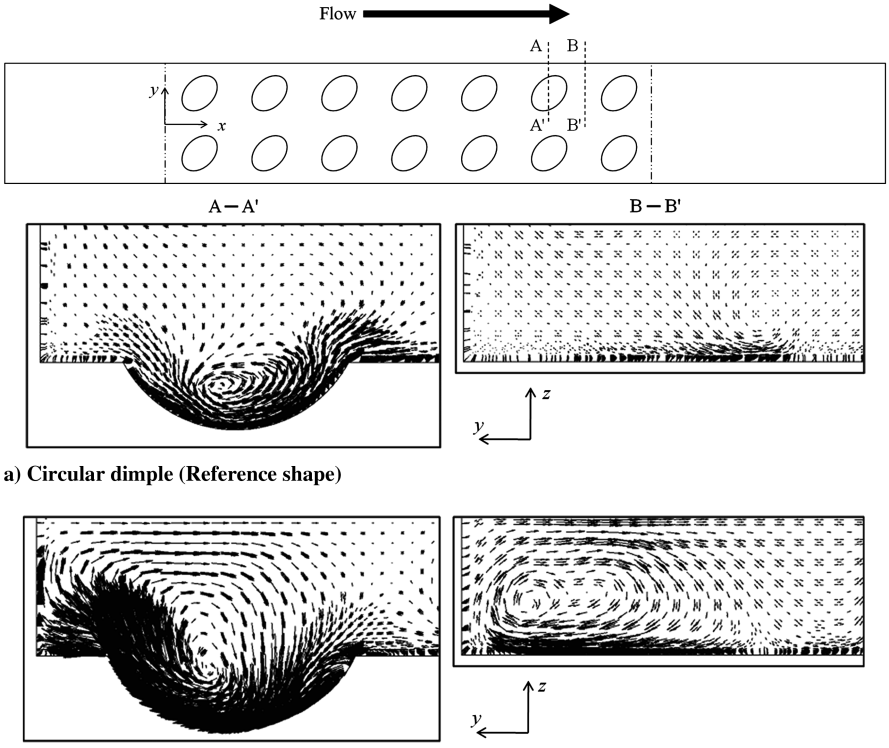

a) Circular dimple (Reference shape)

b) Inclined elliptic dimple (Optimized shape)

Fig. 4 Velocity vector plots at the sixth dimple row.

V. Conclusions

Inclined elliptic dimples in a cooling channel have been optimized using three-dimensional RANS analysis and surrogate-based optimizing techniques to enhance the heat transfer and reduce the pressure drop in the dimpled channel. In an example of the optimization, the heat transfer has been enhanced by 81.2% through the optimization, with 31.7% increment of the pressure drop in the dimpled channel compared with the reference circular dimples. The objective-function value predicted by the RBNN model agrees well with the RANS computed value with 1.3% relative error at the optimum point. The flow structure in the optimum channel indicates that the improvement in the heat transfer performance is induced by a strong vortex that is generated in the dimple and persists downstream of the dimple.

Acknowledgment

This work was supported by the National Research Foundation of Korea, grant no. 20090083510, funded by the Korean government (Ministry of Education, Science and Technology) through Multi-Phenomena CFD Engineering Research Center.

References

[1] Hwang, S. D., Kwon, H. G., and Cho, H. H., "Heat Transfer with Dimple/Protrusion Arrays in a Rectangular Duct with a Low Reynolds Number Range," *International Journal of Heat and Fluid Flow*, Vol. 29, 2008, pp. 916–926. doi:10.1016/j.ijheatfluidflow.2008.01.004

[2] Ligrani, P. M., Mahmood, G. I., Harrison, J. L., Clayton, C. M., and Nelson, D. L., "Flow Structure and Local Nusselt Number Variations in a Channel with Dimples and Protrusion on Opposite Walls," *International Journal of Heat and Mass Transfer*, Vol. 44, 2001, pp. 4413–4425. doi:10.1016/S0017-9310(01)00101-6

[3] Isaev, S. A., and Leont'ev, A. I., "Numerical Simulation of Vortex Enhancement of Heat Transfer Under Conditions of Turbulent Flow Past a Spherical Dimple on the Wall of a Narrow Channel," *High Temperature*, Vol. 41, No. 5, 2003, pp. 665–679. doi:10.1023/A:1026100913269

[4] Moon, S. W., and Lau, S. C., "Turbulent Heat Transfer Measurements on a Wall with Concave and Cylindrical Dimples in a Square Channel," ASME Turbo Expo, Paper GT2002-30208, Amsterdam, 2008.

[5] Park, J., and Ligrani, P. M., "Numerical Predictions of Heat Transfer and Fluid Flow Characteristics for Seven Different Dimpled Surfaces in a Channel," *Numerical Heat Transfer*, Pt. A, Vol. 47, 2005, pp. 209–232. doi:10.1080/10407780590886304

[6] Silva, C., Park, D., Marotta, E. E., and Fletcher, L. S., "Optimization of Fin Performance in a Laminar Channel Flow Through Dimpled Surfaces," *Journal of Heat Transfer*, Vol. 131, No. 2, 2009, Paper 021702. doi:10.1115/1.2994712

[7] Vicente, P. G., Garcia, A., and Viedma, A., "Heat Transfer and Pressure Drop for Low Reynolds Turbulent Flow in Helically Dimpled Tube," *International Journal of Heat and Mass Transfer*, Vol. 45, 2002, pp. 543–553. doi:10.1016/S0017-9310(01)00170-3

[8] Isaev, S. A., Leontiev, A. I., Kornev, N. V., Hassel, E., and Chudnovsky, Y., "Numerical Modeling and Physical Simulation of Vortex Heat Transfer Enhancement Mechanisms over Dimpled Reliefs," *Proceedings of the 14th International Heat Transfer Conference*, Washington, D.C., Aug. 2010.

[9] Kim, K. Y., and Shin, D. Y., "Optimization of a Staggered Dimpled Surface in a Cooling Channel Using Kriging Model," *International Journal of Thermal Sciences*, Vol. 47, 2008, pp. 1464–1472. doi:10.1016/j.ijthermalsci.2007.12.011

[10] Samad, A., Lee, K. D., and Kim, K. Y., "Multi-Objective Optimization of a Dimpled Channel for Heat Transfer Augmentation," *Heat and Mass Transfer*, Vol. 45, 2008, pp. 207–217. doi:10.1007/s00231-008-0420-6

[11] Papila, N., Shyy, W., Griffin, L. W., and Dorney, D. L., "Shape Optimization of Supersonic Turbines Using Response Surface and Neural Network Methods," *Journal of Propulsion and Power*, Vol. 18, 2002, pp. 509–518. doi:10.2514/2.5991

[12] *ANSYS CFX-11.0 Solver Theory*, Ansys, Inc., Canonsburg, PA, 2006.

[13] Menter, F. R., "Two-Equation Eddy-Viscosity Turbulence Models for Engineering Applications," *AIAA Journal*, Vol. 32, No. 8, 1994, pp. 1598–1605. doi:10.2514/3.12149

[14] Samad, A., Shin, D. Y., and Kim, K. Y., "Surrogate Modeling for Optimization of Dimpled Channel to Enhance Heat Transfer Performance," *Journal of Thermophysics and Heat Transfer*, Vol. 21,

No. 3, 2007, pp. 667–670.
doi:10.2514/1.30211

[15] Samad, A., Lee, K. D., and Kim, K. Y., "Multi-Objective Optimization of a Dimpled Channel for Heat Transfer Augmentation," *Heat and Mass Transfer*, Vol. 45, 2008, pp. 207–217.
doi:10.1007/s00231-008-0420-6

[16] McKay, M. D., Beckman, R. J., and Conover, W. J., "A Comparison of Three Methods for Selecting Values of Input Variables in the Analysis of Output from a Computer Code," *Technometrics*, Vol. 21, 1979, pp. 239–245.
doi:10.2307/1268522

[17] Isaev, S. A., and Leont'ev, A. I., "Numerical Simulation of Vortex Enhancement of Heat Transfer Under Conditions of Turbulent Flow Past a Spherical Dimple on the Wall of a Narrow Channel," *High Temperature*, Vol. 41, No. 5, 2003, pp. 665–679.
doi:10.1023/A:1026100913269